



HAL
open science

Impairment of endothelial nitric oxide synthase causes abnormal fat and glycogen deposition in liver

Lorenz Schild, Frank Dombrowski, Uwe Lendeckel, Carla Schulz, Andreas Gardemann, Gerburg Keilhoff

► To cite this version:

Lorenz Schild, Frank Dombrowski, Uwe Lendeckel, Carla Schulz, Andreas Gardemann, et al.. Impairment of endothelial nitric oxide synthase causes abnormal fat and glycogen deposition in liver. *Biochimica et Biophysica Acta - Molecular Basis of Disease*, 2008, 1782 (3), pp.180. 10.1016/j.bbadis.2007.12.007 . hal-00501560

HAL Id: hal-00501560

<https://hal.science/hal-00501560>

Submitted on 12 Jul 2010

HAL is a multi-disciplinary open access archive for the deposit and dissemination of scientific research documents, whether they are published or not. The documents may come from teaching and research institutions in France or abroad, or from public or private research centers.

L'archive ouverte pluridisciplinaire **HAL**, est destinée au dépôt et à la diffusion de documents scientifiques de niveau recherche, publiés ou non, émanant des établissements d'enseignement et de recherche français ou étrangers, des laboratoires publics ou privés.

Accepted Manuscript

Impairment of endothelial nitric oxide synthase causes abnormal fat and glycogen deposition in liver

Lorenz Schild, Frank Dombrowski, Uwe Lendeckel, Carla Schulz, Andreas Gardemann, Gerburg Keilhoff

PII: S0925-4439(07)00237-2
DOI: doi: [10.1016/j.bbadis.2007.12.007](https://doi.org/10.1016/j.bbadis.2007.12.007)
Reference: BBADIS 62774

To appear in: *BBA - Molecular Basis of Disease*

Received date: 27 July 2007
Revised date: 12 December 2007
Accepted date: 13 December 2007



Please cite this article as: Lorenz Schild, Frank Dombrowski, Uwe Lendeckel, Carla Schulz, Andreas Gardemann, Gerburg Keilhoff, Impairment of endothelial nitric oxide synthase causes abnormal fat and glycogen deposition in liver, *BBA - Molecular Basis of Disease* (2007), doi: [10.1016/j.bbadis.2007.12.007](https://doi.org/10.1016/j.bbadis.2007.12.007)

This is a PDF file of an unedited manuscript that has been accepted for publication. As a service to our customers we are providing this early version of the manuscript. The manuscript will undergo copyediting, typesetting, and review of the resulting proof before it is published in its final form. Please note that during the production process errors may be discovered which could affect the content, and all legal disclaimers that apply to the journal pertain.

Impairment of endothelial nitric oxide synthase causes abnormal fat and glycogen deposition in liver

Lorenz Schild¹, Frank Dombrowski², Uwe Lendeckel³, Carla Schulz⁴, Andreas Gardemann¹, and Gerburg Keilhoff⁵

¹Institute of Clinical Chemistry, Department of Pathobiochemistry, Otto-von-Guericke University Magdeburg, Germany

²Institute of Pathology, Ernst-Moritz-Arndt University, Greifswald, Germany

³Institute of Experimental Internal Medicine, Otto-von-Guericke University Magdeburg, Germany

⁴Division of Endocrinology and Metabolic Diseases, University Hospital Magdeburg, Germany

⁵Institute of Medical Neurobiology, Otto-von-Guericke University, Magdeburg, Germany

Corresponding author

Lorenz Schild

Institute of Clinical Chemistry, Department of Pathobiochemistry, Otto-von-Guericke University

Leipziger Str. 44

39120 Magdeburg, Germany

Tel: +49 391 6713644

Fax: +49 391 290176

E-mail adress: lorenz.schild@med.ovgu.de

Key words

Nitric oxide, endothelial nitric oxide synthase, liver, lipids

Summary

Nitric oxide (NO) affects fatty acid synthesis and biogenesis of fatty acid consuming mitochondria. However, whether NO generated by the endothelial NO synthase isoform (eNOS) has significant impact on the synthesis and deposition of fat in liver remained unclear. We analyzed the quantity and distribution of mitochondria and fat in liver of wild type (WT) mice and mice lacking eNOS (eNOS-KO). The livers of eNOS-KO mice contained tenfold more fat close (zone 1) and twenty fold more distal (zone 3) to the artery. The fat was deposited as droplets co-localized with mitochondria. Additionally, the livers of eNOS-KO mice contained 1.5-fold more homogenously distributed glycogen. No difference in the quantity of mitochondria was found between liver homogenates of eNOS-KO mice and WT animals. Mitochondria from liver homogenates of eNOS-KO mice exhibited a higher ratio of citrate synthase (CS) and NADH-cytochrome c-oxidoreductase (KI+III) activity. We conclude that lack of eNOS-derived NO stimulates citrate- and lipid synthesis in liver thus contributing to the development of overweight. In support of this view, more visceral fat and 70% higher body weight was determined in one year old eNOS-KO mice in comparison to WT animals.

Introduction

There are reports that point towards a regulatory effect of NO in lipid metabolism in liver. It has been shown that NO attenuates the synthesis of fatty acids in isolated cultured rat hepatocytes by nitrosylation of acetyl-CoA thereby converting this metabolite to the biologically inactive S-nitroso-CoA [1]. A second mechanism for NO mediated inhibition of fatty acid synthesis is the activation of AMP-activated protein kinase. As a result the cellular level of malonyl-CoA and the activity of fatty acid synthesis are reduced and conversely fatty acid oxidation is stimulated [2]. NO can stimulate AMP-activated protein kinase activity via gene expression [3] and via the generation of peroxynitrite [4]. Additionally, activation of the AMP-activated protein kinase inhibits glycerol-3-phosphate acyltransferase and concomitantly triacylglycerol synthesis [5, 6]. In our own experiments we have demonstrated that NO causes inhibition of fatty acid synthesis in liver at the mitochondrial level. Applying a neuronal NO synthesis knock out (nNOS-KO) model, we have shown that NO contributes to the adjustment of low rates of fatty acid synthesis by limiting citrate synthesis in mitochondria [7]. This could be, at least in part, the mechanism by which the lipid content in liver is regulated. In fact, a lower content of lipids was found in the liver of WT mice in comparison to nNOS-KO mice but without any consequence on body weight [7].

Stimulation of mitochondrial biogenesis by endogenous NO has been reported for several tissues including liver [8]. It has been suggested that an increase in the number of mitochondria enhances energy production thus promoting the oxidation of fatty acids. In line with this hypothesis is the observation by the authors that WT mice had a significantly lower body weight than eNOS-KO mice. However, an increase in energy turnover would require a higher energy demand. Currently, there is no convincing evidence for a metabolically founded higher energy demand in WT mice versus eNOS-KO mice. Moreover, it is still unclear whether NO originated from eNOS is involved in the regulation of lipid deposition in liver and how mitochondria contribute to this process.

In order to investigate the effect of NO generated by eNOS on mitochondria we determined not only the quantity but also the distribution of mitochondria in the livers of WT mice and eNOS-KO mice by applying electron microscopy analysis. The cellular amount of mitochondria was independently estimated by determining the ratio of nuclear and mitochondrial DNA in liver homogenates of WT and eNOS-KO mice. Furthermore, we investigated whether mitochondria from the livers of WT and eNOS-KO mice differ in their enzymatic composition. In this context we focused on the determination of the activities of CS and KI+III since an excess of citrate can serve as substrate for cytosolic fatty acid synthesis.

We have found significant differences in the ratio of the activities of both enzymes as well as in the local distribution of mitochondria in the livers between WT and eNOS-KO mice but not in the amount of mitochondria. The next series of experiments was aimed to analyze the content and local distribution of fat and glycogen in the livers of WT and eNOS-KO mice. The livers of eNOS-KO mice contained much more glycogen and fat. The latter was inhomogeneously distributed and found predominantly localized in zone 3 (distal to the artery) according to Rappaport's nomenclature. Finally, we searched for systemic consequences of the NO-dependent distribution of mitochondria, glycogen and fat in liver by measuring body weight as well as insulin, triacylglycerol, and glucose in the blood of WT and eNOS-KO mice. Differences were found in body weight, insulin and glucose levels but not in the triacylglycerol content between WT and eNOS-KO mice. Our data suggest that the impact of NO on mitochondria contributes in the control of lipid metabolism in liver and body weight.

Methods

Animals

The experiments were performed using male laboratory bred homozygous eNOS-KO (C57BL/6 background) and nNOS-KO (C57BL/6,129S background) mice [9, 10] and WT mice (C57BL/6 background). All animals were maintained at 21°C in accordance with the guidelines of the German Animal Welfare Act. The experimental protocol was approved by a review committee of the state of Sachsen-Anhalt, Germany. With exception of age dependent investigations 120-140 day old animals were used. For the study, the mice were sacrificed by decapitation or by overdosed anesthesia with pentobarbital intraperitoneally.

Histological analysis

The livers were removed and fixed either in 3% paraformaldehyde for paraffin embedded H & E sections or Sudan red stained frozen sections, or they were fixed in 2.5% glutaraldehyde and OsO₄ for Epon 812 embedded semithin and thin sections. Semithin sections were stained according to Richardson [11], ultrathin sections were stained with lead citrate and uranyl acetate, and examined with a Zeiss EM900 electron microscope. For the determination of the volume fractions occupied by mitochondria, fat and glycogen the stereological method of Weibel was used [12]. At least 600 points were analyzed for the calculation.

Preparation of liver homogenates

The extracted tissues were minced using small scissors and transferred into ice cold phosphate buffer solution (PBS) at pH 7.4. Subsequently, the tissues were homogenized at 4 °C using a Potter-Elvehjem glass-teflon homogenizer performing 10 strokes at 600 rpm. After determination of protein, all samples were adjusted to identical protein content by adding adequate amounts of PBS.

Determination of protein

The protein content of the samples was determined by the Pierce bicinchoninic acid protein assay [13] using bovine serum albumin as the standard.

Determination of citrate synthase activity (EC 2.3.3.1)

Citrate synthase activity was assayed using a standard procedure at 30 °C [14]. Homogenate samples of respective tissues (40 µg) were evaluated. The decrease of acetyl CoA absorption

was monitored at 412 nm using a Cary 1E spectral photometer (Varian). The reaction mixture contained 100 mM Tris-HCl buffer (pH 8.0), 5 mM MgCl₂, 0.5 mM 5,5-dithio-bis-2-nitrobenzoic acid (DTNB), 0.2 mM acetyl CoA, and 1 mM oxaloacetic acid.

Determination of NADH:cytochrome c oxidoreductase activity (EC 1.6.99.3)

Samples of 500 µl were drawn from the homogenates. The mitochondria were disintegrated by sonication. A 15 µl volume (40 µg protein) was used to run the assay at 30 °C as described in [13]. The reduction of cytochrome c was followed by measurement of the absorption at 550 nm with a Varian spectrophotometer (Cary 1E). The rotenone-sensitive absorption was used for quantification.

Mitochondrial / nuclear DNA ratio

Determination of the ratio between mitochondrial and nuclear DNA contents was performed by quantitative real-time PCR, essentially as described by others [16, 17]. For DNA isolation, whole tissue samples from each eight wild-type and eNOS^{-/-} mice were powdered in liquid nitrogen and 25 mg aliquots were used for DNA extraction by means of the QIAamp DNA Mini Kit (Qiagen, Hilden, Germany). For each DNA extract, the nuclear gene for ribosomal protein large p0 and the mitochondrial gene cytochrome-c oxidase subunit I (CoxI) were quantified separately by real-time PCR using the iCycler (Bio-Rad, Munich, Germany). The PCR reactions were performed in triplicate for each gene. A typical 25-µl reaction mixture contained 12.5 µl HotStarTaq Master Mix (Qiagen), 0.3 µl of a 1:1000 dilution of SYBR Green I (Molecular Probes, Eugene, Oregon), 100 ng DNA, and 0.5 µmol of the specific primers: *p0-US* 5'-GCACITTCGCTTCTGGAGGGTGT-3' and *p0-DS* 5'-TGACTTGTTGCTTTGGCGGGATT-3'; *CoxI-US* 5'-TCTACTATTTCGGAGCCTGAG-3' and *CoxI-DS* 5'-CTACTGATgCTCCTGCATGG-3'. An initial denaturation/activation step (15 min 95 °C) was followed by 40 cycles (30 s 95 °C, 30 s 58 °C, 45 s 72 °C).

Determination of triacylglycerol

The content of triacylglycerol in the serum was determined according to [18]. The serum from non-fasted WT and eNOS-KO mice was obtained by centrifugation for 10 minutes at 3000 x g. All blood samples were collected in the morning within 30 minutes. Subsequently the

samples were hydrolyzed with ethanolic KOH (0.5 M) and after 30 minutes of incubation at 70 °C neutralized (pH 7) with perchloric acid (2.5 M). The content of glycerol of 100 µl samples was determined in a reaction mixture with a final volume of 1 ml containing: 71.4 mM triethanolamine, 8.5 mM Mg²⁺, 1.0 mM phosphoenolpyruvate, 0.4 mM NADH, 2.0 mM ATP, 5 units pyruvate kinase, 5 units lactate dehydrogenase and 0.5 units glycerol kinase. The absorption of NADH was measured at room temperature with a Varian spectrophotometer (Cary 1E) at a wavelength of 340 nm. For the calculation of triacylglycerol content the difference of free and bound glycerol was used.

Determination of glucose

Serum samples from trunk blood were collected at sacrifice. Blood glucose was determined immediately after sacrifice with a Biosen 5030 glucose analyzer (EKF-diagnostic GmbH, Barleben/Magdeburg, Germany) employing the glucose oxidase method as principle of measurement.

Determination of insulin

Serum insulin concentration was determined by means of a commercial radioimmuno-assay (RIA) suitable for mouse insulin (Rat Insulin RIA Kit, LINCO Research, St. Charles, MO, USA). All determinations were performed in duplicate; the manufacturer's protocol was adapted to smaller sample sizes.

Statistical analysis

Statistical analysis was carried out with ANOVA test with two-way layout combined with post hoc Tekey test. For the comparison of parameters from eNOS-KO mice and WT mice unpaired Student's *t* test was used. Detailed information is given in the legends of Figures and Tables. Data is presented as means ± SEM. Statistical analysis of differences with $p < 0.05$ was taken as the indicator of significance.

Results

Endogenous NO from eNOS controls distribution and enzymatic pattern of liver mitochondria

To study the effect of endogenous NO originated from eNOS on mitochondria in liver, we first analyzed the ratio between mitochondrial and nuclear DNA by applying real-time PCR.

This ratio reflects the quantity of mitochondria per cell. In contrast to Nisoli et al. [8], we did not find any significant difference in the amount of mitochondria by comparing the ratio of mitochondrial and nuclear DNA in liver homogenates from WT and eNOS-KO mice (triplicates from three animals per mouse model), (WT: 54.08 ± 2.02 versus eNOS-KO: 53.63 ± 1.57). Additionally, we applied electron microscopic analysis in order to determine the distribution of mitochondria within the hepatocytes. Electron micrographs from hepatocytes of WT, nNOS-KO, and eNOS-KO mice are presented in Fig. 1. Since the local concentration of NO results from different sources the liver of nNOS-KO mice was included in the analysis (Fig. 1B). Fat deposition in form of droplets (indicated with asterisks) is seen in the cytosol of hepatocytes of WT and eNOS-KO mice but not in the liver of nNOS-KO mice. It is remarkable that mitochondria (arrow heads) and fat drops are clearly co-localized (Fig. 1A and 1C). The detailed analysis of the areas of the cytosol (without glycogen and fat) that are occupied by mitochondria revealed a clear distribution of mitochondria within the tissue (table 1). We found no significant difference in the quantity and distribution of mitochondria between WT and nNOS-KO mice. However, the livers of eNOS-KO mice contained in zone I which is closest to the artery (according to Rappaport's nomenclature) significantly less and in zone 3 (distal to the artery) more mitochondria than the liver of WT animals.

In the next series of experiments we investigated whether mitochondria from WT and eNOS-KO mice differ in their enzymatic pattern. Since citrate produced in the mitochondrial matrix can serve as substrate for cytosolic fatty acid synthesis the relationship between the activities of the citric acid cycle and the respiratory chain was analyzed. Therefore, the activity of CS and KI+III was determined from liver homogenates of WT and eNOS-KO mice. The liver homogenates of WT mice had higher activities of CS and KI+III in comparison to eNOS-KO mice (Table 1). However, the ratio of CS activity and KI+III activity was significantly higher in the homogenates of eNOS-KO mice (0.279 ± 0.019 for eNOS-KO versus 0.208 ± 0.021 for WT). Although these data from the tissue homogenates do not reflect specificities of liver architecture it may be suggested that the relative excess of citric acid cycle enzymes promotes fatty acid synthesis in eNOS-KO mice.

Endogenous NO from eNOS determines fat and glycogen deposition in liver

On the basis of these findings we were interested to investigate the deposition of fat in liver from WT, nNOS-KO, and eNOS-KO mice. For this purpose thin tissue slices were prepared and analyzed by light microscopy. The staining according to Richardson revealed massive fat deposition in zone 3 of the liver from eNOS-KO mice (Fig. 2C) whereas no such fat deposits were observed in the livers of WT and nNOS-KO mice (Fig. 2A and B). Massive fat deposition in zone 3 of livers from eNOS-KO mice was confirmed by the fat-specific Sudan red staining (Fig. 2D).

Electron micrographs of the livers were statistically analyzed for the quantification of fat deposition. The volume fraction of the entire cytosol (without nucleus) occupied by the membranous fat droplets was determined. The relative volumes of the fat deposits in zone 1 and zone 3 of the livers of WT and eNOS-KO mice are presented in Fig. 3A. To give an impression of the fat deposition in the tissue the mean of zone 1 and 3 are given additionally. These mean values reveal a massive fat deposition in the liver of eNOS-KO mice in comparison to WT mice (33.58 ± 1.94 % of cytosol area in eNOS-KO versus 1.66 ± 0.79 % of cytosol area in WT mice). The fat in the liver of eNOS-KO mice was predominantly localized in zone 3 (10.87 ± 0.69 % of cytosol area in zone 1 versus 56.30 ± 3.27 % of cytosol area in zone 3). Accordingly, the accumulation of fat was higher in zone 3 than in zone 1 with respect to WT mice (zone 1: 0.833 ± 0.48 % of cytosol area in WT versus 10.87 ± 0.69 % of cytosol area in eNOS-KO mice; zone 3: 2.50 ± 1.12 % of cytosol area in WT versus 56.30 ± 3.27 % of cytosol area in eNOS-KO mice).

Accumulation of glycogen was found in the liver of eNOS-KO mice predominantly in zone 1 (Fig. 3B, zone 1: 30.9 ± 1.5 % of cytosol area in eNOS-KO versus 17.8 ± 0.6 % of cytosol area in WT, $p=0.007$). This effect was observed in tendency also in zone 3 (Fig. 3B, zone 3: 26.0 ± 2.0 % of cytosol area in eNOS-KO versus 21.4 ± 0.3 % of cytosol area in WT, $p=0.49$). However, no significant difference in the cellular content of glycogen between zone 1 and zone 3 could be detected in the livers of eNOS-KO mice and WT mice. A significant difference in the content of glycogen between zone 1 and 3 was only determined in nNOS-KO mice (10.3 ± 0.8 % of cytosol area in zone 1 versus 17.2 ± 0.8 % of cytosol area in zone 3, $p=0.025$). Taken the average glycogen content of zone 1 and 3 as a representative of the tissue glycogen, the livers of eNOS-KO mice contained about 1.5 fold more glycogen in comparison to WT mice. The homogenous distribution of glycogen in the liver of eNOS-KO mice suggests that glycogen metabolism does not sensitively depend on local NO in this range of concentration.

Impairment of eNOS is associated with increase in visceral fat and lower serum levels of glucose and insulin

Since massive fat deposition was found in the liver of eNOS-KO mice we investigated the amount of fat in the abdominal depot in WT and eNOS-KO mice. The comparison of 12 month old WT and eNOS-KO mice revealed a much higher amount of visceral fat in eNOS-KO mice (Fig. 4). Moreover, it is evident that eNOS-KO mice are bigger in comparison to WT animals. To provide a quantitative parameter for this observation we determined the body weight. The body weight of male WT, nNOS-KO, and eNOS-KO mice in dependence on age is presented in Fig. 5. The impairment of nNOS was without consequences on the body weight. However, loss of eNOS expression was associated with a 1.6 fold higher body weight of eNOS-KO mice at the age of one year. The difference in body weight of WT and nNOS-KO mice versus eNOS-KO mice evolved continuously with growing age. From the finding that eNOS-KO mice but not nNOS-KO mice had a higher body weight in comparison to WT mice it may be concluded that eNOS contributes more to the local NO concentration in several tissues than nNOS does.

Although massive accumulation of fat was found in the liver and abdomen in eNOS-KO mice we determined equal concentrations of triacylglycerol in the blood of WT and eNOS-KO mice (Table 2). Obviously, the capacity of fat depots and lipid transport system was not yet exceeded. In contrast, the blood of eNOS-KO mice contained less glucose (7.63 ± 0.69 mmol/l in eNOS-KO mice versus 9.44 ± 0.71 mmol/l in WT mice) and insulin (0.63 ± 0.23 ng/ml in eNOS-KO mice versus 1.68 ± 0.51 ng/ml in WT mice) in comparison to WT mice.

Discussion

It had been reported that NO is involved in the regulation of biogenesis of mitochondria in several tissues such as brain, heart, brown adipose tissue, and even in liver. This conclusion was based on the finding that long term caloric restriction causes increase of eNOS protein as well as the mitochondrial proteins cytochrome c oxidase subunit IV and cytochrome c in WT mice but not in eNOS-KO mice [19]. Increase of these mitochondrial proteins was also found in several cell types treated with a NO donor [8]. Moreover, effects of NO on the biogenesis

of mitochondria in rat skeletal muscle had been demonstrated [20]. We did not find differences in the ratio of mitochondrial and nuclear DNA in liver homogenates by using real time PCR neither between WT and nNOS-KO mice [7] nor between WT mice and eNOS-KO mice. This ratio is a measure of the cellular content of mitochondria. Electron microscopic analysis revealed that mitochondria were homogeneously distributed in the liver of WT and nNOS-KO mice whereas structure-dependent distribution of mitochondria in the liver of eNOS-KO mice was found. The content of mitochondria was low close to the artery (zone 1) and high in the neighborhood of the central vein (zone 3).

It had been demonstrated that NO directly affects mitochondrial metabolism. NO inhibits electron transport within the respiratory chain at the level of the cytochrome c oxidase [21]. Further, inhibition of the mitochondrial aconitase by NO had been reported [22, 23]. In our previous work we have shown that NO is additionally involved in the regulation of the expression of mitochondrial enzymes. We have found different activities of respiratory chain complexes and citrate synthase in WT and nNOS-KO mice [7]. Likewise, we now report about different activities of CS and KI+III in eNOS-KO and WT mice. In contrast to nNOS-KO mice, mitochondria are not homogeneously distributed across the liver of eNOS-KO mice. Therefore, it may be speculated that the enzymatic pattern of mitochondria differs in dependence on the liver architecture. Our data determined in liver homogenates do not reflect structural specialties of the tissue and therefore may underestimate differences in the activities of mitochondrial enzymes between WT and eNOS-KO mice.

An essential result of our work is the documentation of massive fat deposition in the liver of eNOS-KO mice. The fat was found within the hepatocytes as membraneless fat droplets in association with mitochondria. Moreover, the distribution of fat clearly correlated with the distribution of mitochondria in the liver of eNOS-KO mice. From these findings we suggest that mitochondria are involved in fatty acid synthesis in hepatocytes. Similar to mitochondria analyzed in liver homogenates of nNOS-KO mice increase in the ratio of the activities of citrate synthase and NADH-cytochrome c oxidoreductase was determined even in liver homogenates of eNOS-KO mice in comparison to liver homogenates of WT mice. However, this ratio differed less between eNOS-KO and WT than between nNOS-KO and WT [7]. This may result from the in-homogenous distribution of mitochondria and fat in the livers of eNOS-KO mice. The local excess of citrate would result in increased cytosolic citrate concentration via the transport through the mitochondrial membrane. This may cause stimulation of acetyl-CoA formation by the ATP-dependent citrate lyase. Citrate lyase is a

key enzyme of fatty acid metabolism. Therefore, fatty acid synthesis may be stimulated by increased generation of citrate within the mitochondria. This may explain the local association of mitochondria and fat droplets within the hepatocytes and over the entire organ. As a second aspect, it is reasonable to assume that the local concentration of oxygen in liver differs between WT and eNOS-KO mice. In the liver of WT mice the oxygen concentration is relatively high far away from the artery (zone 3) since close to the artery (zone 1) the mitochondrial oxygen consumption is limited due to NO-dependent inhibition of cytochrome c oxidase. In contrast, in the liver of eNOS-KO mice the oxygen concentration in zone 3 is low since some of the oxygen is consumed by the mitochondria in zone 1. In the liver of eNOS-KO mice the citric acid cycle may generate more citrate that can be used for fatty acid synthesis because restricted oxygen supply in zone 3 reduces the activity of the electron transport chain. Besides changes in the enzymatic pattern of mitochondria this may explain the structured distribution of fat deposits in the liver of eNOS-KO mice. In our previous report [7] we demonstrated accumulation of total lipids in the livers of nNOS-KO mice in comparison to WT mice. This increase in total lipids was not accompanied by higher triacylglycerol and body weight (earlier own results, Fig. 5). Increase in total lipids which are represented by free fatty acids, phospholipids and triacylglycerol but not exclusively in triacylglycerol may reflect a moderate drop in local NO concentration as can be reached by knocking out nNOS. The observation that knocking out eNOS in mice causes the architecture-dependent massive accumulation of fat in liver may underline the dominant contribution of eNOS to local NO concentration.

To study the zone-dependent lipid metabolism in the liver of eNOS-KO mice in detail, hepatocytes or mitochondria from the zones of the liver that display massive fat accumulation have to be isolated. This separation would allow the comparison of cytosolic accumulation of citrate and acetyl-CoA in zone 3 and zone 1. Evaluation of nitrosilation of acetyl CoA is of great interest when values of zone 3 and zone 1 are compared additionally between eNOS-KO mice and WT mice. The same material of the livers would be required in order to provide conclusive data for a possible NO-dependent activation of AMP-activated protein kinase in these mouse models. To date, suitable methods with an adequate yield for the isolation of hepatocytes and mitochondria from separate liver zones are not available.

We have also found higher amounts of glycogen deposits in zone 1 and 3 of livers from eNOS-KO mice in comparison to WT mice. It is known that NO dose-dependently inhibits gluconeogenesis [24] and glycogen synthesis at the level of the glycogen synthase [25] in

hepatocytes. The effect of NO on gluconeogenesis is mediated by the activation of AMP-activated protein kinase [26]. The accumulation of glycogen in the liver of eNOS-KO mice is consistent with the lack of NO-inhibition on carbohydrate metabolism.

Besides deposition of high amounts of fat in liver, eNOS-KO mice exert massive accumulation of visceral fat obviously contributing to higher body weights in comparison to WT mice. The difference in body weight between eNOS-KO and WT mice increased with age. Similar results were obtained in other laboratories. At the age of 10 month, eNOS-KO mice have been found to be 48 % heavier than WT mice [27] whereas at lower ages between 8-16 weeks either no [28, 29] or small differences in body weight were observed [30]. Higher body weights of eNOS-KO mice in comparison to WT mice were also reported by Nisoli et al. [8], but were mainly attributed to low energy turn over due to less mitochondria. In comparison to the data of Nisoli et al. [8] our mice grew slower. A reason for this discrepancy may be different environmental conditions. The animals of the report of these authors were maintained at 24°C whereas our animals were held at 21°C. Here we report for the first time that NO-dependent fat deposition is linked to mitochondrial metabolism in liver. This conclusion is based on the co-localization of mitochondria and fat droplets, the distribution of fat and mitochondria in dependence on the distance to the artery, and changes in the ratio of the citrate synthase and NADH-cytochrome c oxidoreductase activities. In contrast to Nisoli et al. [8], we did not find differences in the quantity of liver mitochondria between WT and eNOS-KO mice. One reason for this discrepancy may be the different temperature at which the animals were maintained.

Despite higher body weight, more visceral fat, and massive fat deposition in the liver of eNOS-KO mice, we found similar serum levels of triacylglycerol in WT and eNOS-KO mice. Obviously, the capacity of the transport system for triacylglycerol is not yet overloaded. In contrast, our data reveal that serum insulin and glucose levels are lower in eNOS-KO mice. In this context we speculate that the synthesis of glycogen and triacylglycerol requires an increased ATP production. In turn, this would cause acceleration of glucose consumption resulting in lower serum glucose concentration combined with decrease in insulin secretion.

It had been shown that NO is involved in the regulation of the metabolism of glucose, fatty acids and amino acids in mammals. A number of regulatory sites had been identified [31]. With our data we add a yet unrecognized mechanism to the NO-dependent regulation of lipid metabolism. It is the control of the activity of mitochondrial enzymes which are involved in fatty acid synthesis, namely CS and KI+III. Furthermore, our data reveal that a defect in NO

generation by eNOS contributes to the development of overweight and obesity. Obesity is a major risk factor for insulin resistance, type II diabetes, atherosclerosis, stroke, hypertension, impaired vascular function, sleep disorders and some types of cancer [32].

Acknowledgements

We thank Silke Niemann and Leona Bück for excellent assistance as well as Dr. Siegfried Kropf for the statistical analysis. This work was supported by the Bundesministerium für Bildung und Forschung (NBL3, PP4).

References

- [1] W.E. Roediger, R. Hems, D. Wiggins, G.F. Gibbons, Inhibition of hepatocyte lipogenesis by nitric oxide donor: could nitric oxide regulate lipid synthesis? *IUBMB Life* 56 (2004) 35-40.
- [2] W.W. Winder, D.G. Hardie, Inactivation of acetyl-CoA carboxylase and activation of AMP-activated protein kinase in muscle during exercise, *Am. J. Physiol.* 270 (1996) E299-E304.
- [3] W.J. Fu, T.E. Haynes, R. Kohli, J. Hu, W. Shi, T.E. Spencer, R.J. Carroll, C.J. Meininger, G. Wu, Dietary L-arginine supplementation reduces fat mass in Zucker diabetic fatty rats, *J. Nutr.* 135 (2005) 714-21.
- [4] M.H. Zou, X.Y. Hou, C.M. Shi, S. Kirkpatrick, F. Liu, M.H. Goldman, R.A. Cohen, Activation of 5'-AMP-activated kinase is mediated through c-Src and phosphoinositide 3-kinase activity during hypoxia-reoxygenation of bovine aortic endothelial cells. Role of peroxynitrite, *J. Biol. Chem.* 278 (2003) 34003-10.
- [5] H. Park, V.K. Kaushik, S. Constant, M. Prentki, E. Przybytkowski, M.B. Ruderman, A.K. Saha, Coordinate regulation of malonyl-CoA decarboxylase, sn-glycerol-3-phosphate acyltransferase, and acetyl-CoA carboxylase by AMP-activated protein kinase in rat tissues in response to exercise, *J. Biol. Chem.* 277 (2002) 32571-7.
- [6] D.M. Muoio, K. Seefeld, L.A. Witters, R.A. Coleman, AMP-activated kinase reciprocally regulates triacylglycerol synthesis and fatty acid oxidation in liver and muscle: evidence that sn-glycerol-3-phosphate acyltransferase is a novel target, *Biochem. J.* 338 (1999) 783-91.
- [7] L. Schild, I. Jaroscakova, U. Lendeckel, G. Wolf, G. Keilhoff, Neuronal nitric oxide synthase controls enzyme activity pattern of mitochondria and lipid metabolism, *FASEB J.* 20 (2006) 145-7.
- [8] E. Nisoli, E. Clementi, C. Paolucci, V. Cozzi, C. Tonello, C. Sciorati, R. Bracale, A.

- Valerio, M. Francolini, S. Moncada, M.O. Carruba, Mitochondrial biogenesis in mammals: the role of endogenous nitric oxide, *Science* 299 (2003) 896-9.
- [9] P.L. Huang, T.M. Dawson, D.S. Brecht, S.H. Snyder, M.C. Fishman, Targeted disruption of the neuronal nitric oxide synthase gene, *Cell* 75 (1993) 1273-86.
- [10] J.E. Brenman, H. Xia, D.S. Chao, S.M. Black, D.S. Brecht, Regulation of neuronal nitric oxide synthase through alternative transcripts, *Dev. Neurosci.* 19 (1997) 224-31.
- [11] K.C. Richardson, L. Jarret, E.H. Finke, Embedding in epoxy resins for ultrathin sectioning in electron microscopy, *Stain Technol.* 35 (1960) 313.
- [12] E.R. Weibel, Stereological principles for morphometry in electron microscopic cytology, *Int. Rev. Cytol.* 26 (1969) 235-302
- [13] K. Wiechelmann, R. Braun, J. Fitzpatrick, Investigation of the bicinchoninic acid protein assay: identification of the groups responsible for color formation. *Anal. Biochem.* 175 (1988) 231-237.
- [14] P.A. Srere, *Methods in Enzymology*, Editors: S.P. Colowick, N.O. Kaplan, Academic Press, 13 (1969) 3-11.
- [15] M.A. Birch-Machin, H.L. Briggs, A.A. Saborido, L.A. Bindoff, D.M. Turnbull, Na evaluation of the measurement of the activities of complexes I-IV in the respiratory chain of human skeletal muscle mitochondria, *Biochem. Med. Metab. Biol.* 51 (1994) 35-42.
- [16] H.C.F. Cote, Z.L. Brumme, K.J.P. Craib, C.S. Alexander, B. Wynhoven, L. Ting, H. Wong, M. Harris, R. Harrigan, M.V. O'Shaughnessy, J.S.G. Montaner, Changes in mitochondrial DNA as a marker of nucleoside toxicity in HIV-infected patients, *N. Engl. J. Med.* 346 (2002) 811-820.
- [17] M.M. Kim, J.D. Clinger, B.G. Masayeva, P.K. Ha, M.L. Zahurak, W.H. Westra, J.A. Califano, Mitochondrial DNA quantity increases with histopathologic grade in premalignant and malignant head and neck lesions, *Clin. Canc. Res.* 10 (2004) 8512-8515.
- [18] H.U. Bergmeyer (ed), *Methoden der enzymatischen Analyse*. Weinheim, Verlag Chemie, (1974) 1878-1878.
- [19] E. Nisoli, C. Tonello, A. Cardile, V. Cozzi, R. Brancale, L. Tedesco, S. Falcone, A. Valerio, O. Cantoni, E. Clementi, S. Moncada, M.O. Carruba, Calorie restriction promotes mitochondrial biogenesis by inducing the expression of eNOS, *Science* 310

- (2005) 314-7.
- [20] G.C. Wadley, G.K. McConnell, Effect of nitric oxide synthase inhibition on mitochondrial biogenesis in rat skeletal muscle, *J. Appl. Physiol.* 102 (2007) 314-320.
- [21] G.C. Brown, V. Borutaite, Nitric oxide, cytochrome c and mitochondria. *Bioch. Soc. Symp.* 66 (1999) 17-25.
- [22] J.C. Drapier, Interplay between NO and [Fe-S] clusters: relevance to biological systems, *Methods* 11 (1997) 319-329.
- [23] V. Tortora, C. Quijano, B. Freeman, R. Radi, L. Castro, Mitochondrial aconitase reaction with nitric oxide S-nitrosoglutathione, and peroxynitrite: Mechanisms and relative contributions to aconitase inactivation, *Free Radic. Biol. Med.* 42 (2007) 1075-1088.
- [24] R.A. Horton, E.D. Ceppi, R.G. Knowles, M.A. Titheradge, Inhibition of hepatic gluconeogenesis by nitric oxide: a comparison with endotoxic shock, *Biochem. J.* 299 (1994) 735-739.
- [25] F. Sprangers, H.P. Sauerwein, J.A. Romijn, G.M. van Woerkom, A.J. Meijer, Nitric oxide inhibits glycogen synthesis in isolated rat hepatocytes, *Biochem. J.* 330 (1998) 1045-9.
- [26] B.B. Kahn, T. Aquier, D. Carling, D.G. Hardie, AMP-activated protein kinase ancient energy gauge provides clues to modern understanding of metabolism, *Cell Metab.* 1 (2005) 15-25.
- [27] I. Momken, P. Lechéne, R. Ventura-Clapier, V. Veksler, Voluntary physical activity alterations in endothelial nitric oxide synthase knockout mice, *Am. J. Heart Circ. Physiol.* 287 (2004) 914-920.
- [28] G. D. Wadley, J. Choate, G. K. McConnell, NOS isoform-specific regulation of basal but not exercise-induced mitochondrial biogenesis in mouse skeletal muscle, *J. Physiol.* 585 (2007) 253-262.
- [29] T. Morishita, M. Tsutsui, H. Shimokawa, K. Sabanai, H. Tasaki, O. Suda, S. Nakata, A. Tanimoto, K. Y. Wang, Y. Ueta, Y. Sasaguri, Y. Nakashima, N. Yanagihara, Nephrogenic diabetes insipidus in mice lacking all nitric oxide synthase isoforms, *PNAS* 102 (2005) 10616-10621.
- [30] N. Kubis, C. Richer, V. Domergue, J. F. Giudicelli, B. I. Lévy, Role of microvascular rarefaction in the increased arterial pressure in mice lacking for the endothelial nitric oxide synthase gene (eNOS^{-/-}), *J. Hypertens.* 20 (2002) 1581-1587

- [31] W.S. Jobgen, S.K. Fried, F.J. Wenjiang, C.J. Meininger, G. Wu, Regulatory role for the arginine-nitric oxide pathway in metabolism of energy substrates, *J. Nutr. Biochem.* 17 (2006) 571-588.
- [32] E. Nisoli, M.O. Carruba, Emerging aspects of pharmacotherapy for obesity and metabolic syndrome, *Pharmacol. Res.* 50 (2004) 453-609.

Legends

Fig. 1

Effect of endogenous NO on the distribution of fat and mitochondria in hepatocytes. Electron micrographs of the liver from acinar zone 3 (according to Rappaport) of WT mice (A), zone 1 of nNOS-KO mice (B), zone 3 of eNOS-KO mice (C), and zone 1 of eNOS-KO mice (D) are shown. In all cases the same magnification was used. The length of the bar corresponds to 1 μm . Fat deposits in form of membraneless droplets (asterisks) were predominantly found in zone 3. Mitochondria (arrow heads) were co-localized with the fat droplets.

Fig. 2

Effect of endogenous NO on fat deposition in liver tissue. Semithin sections stained according to Richardson (A-C) or Sudan red stained kryo-sections (D) were prepared for histological analysis of the livers from WT, nNOS-KO, and eNOS-KO mice. The width of the pictures corresponds to 810 μm . **A:** WT; **B:** nNOS-KO; **C:** e-NOS-KO; **D:** eNOS-KO. Massive fat deposition is documented in zone 3 of the livers only from eNOS-KO mice.

Fig. 3

Effect of eNOS-derived NO on the distribution of fat and glycogen in liver. Areas of the cytosol (without nucleus) occupied by fat or glycogen are determined in electron micrographs of liver from WT, nNOS-KO and eNOS-KO mice. Zone 1 and zone 3 were analyzed. Additionally, mean values of zone 1 and zone 3 (zone 1 + zone 3) are presented. Data were accumulated from 3 animals per group and were presented as mean \pm SEM. Statistical analysis was performed using ANOVA for repeated measurements considering zones as within-factor and genotypes as between-factor. Tukey test for pair wise comparison of genotype was used as post hoc test. Additionally, differences between zone 1 and 3 were separately tested using simple paired t-test. *difference is significant for eNOS-KO versus WT and eNOS-KO versus nNOS-KO for zone 1; ** difference is significant for eNOS-KO versus WT and eNOS-KO versus nNOS-KO for zone 3; + difference is significant for eNOS-KO versus WT and eNOS-KO versus nNOS-KO for zone 1 plus zone 3; ++ difference is

significant between zone 1 and zone 3 in eNOS-KO mice. # difference is significant for eNOS-KO versus WT, eNOS-KO versus nNOS-KO, and nNOS-KO versus WT for zone 1; ## difference is significant for eNOS-KO versus WT and eNOS-KO versus nNOS-KO for zone 1 plus zone 3; § difference is significant between zone 1 and zone 3 in nNOS-KO mice.

Fig. 4

Effect of eNOS-derived NO on the accumulation of visceral fat. One year old WT mouse (left) is compared with equal aged eNOS-KO mouse (right).

Fig. 5

Effect of endogenous NO on body weight. The body weight of male WT, nNOS-KO, and eNOS-KO mice was recorded in dependence on time. Five animals of each group were analyzed. Data are presented as mean \pm SEM. Statistical analysis was performed using ANOVA with two-way layout with the factors age and genotype and Tukey test as post hoc test for both factors. The difference of body weight was significant with $p < 0.05$ at all ages (3, 4, and 12 month) for eNOS-KO versus WT mice and eNOS-KO versus nNOS-KO mice (asterisks). Each genotype grew significantly from point to point of observation.

Table 1

Effect of eNOS-derived NO on the distribution and enzymatic pattern of mitochondria in liver. The distribution of mitochondria was analyzed on the base of electron micrographs. Three animals per group were evaluated for this investigation. For the determination of the activities of CS and KI+III liver homogenates were prepared. Five livers were used for each group. The data are presented as mean \pm SEM. Differences between parameters of eNOS-KO and WT mice were analysed by applying unpaired Student's *t* test. *difference between WT and eNOS-KO mice is significant with $p < 0.05$.

Table 2

Effect of eNOS-derived NO on serum levels of glucose, triacylglycerol, and insulin. Serum samples from trunk blood were collected at sacrifice. Five animals of each group were analyzed. The data are presented as mean \pm SEM. Differences between parameters of eNOS-KO and WT mice were analysed by applying unpaired Student's *t* test. *difference between WT and eNOS-KO mice is significant with $p < 0.05$.

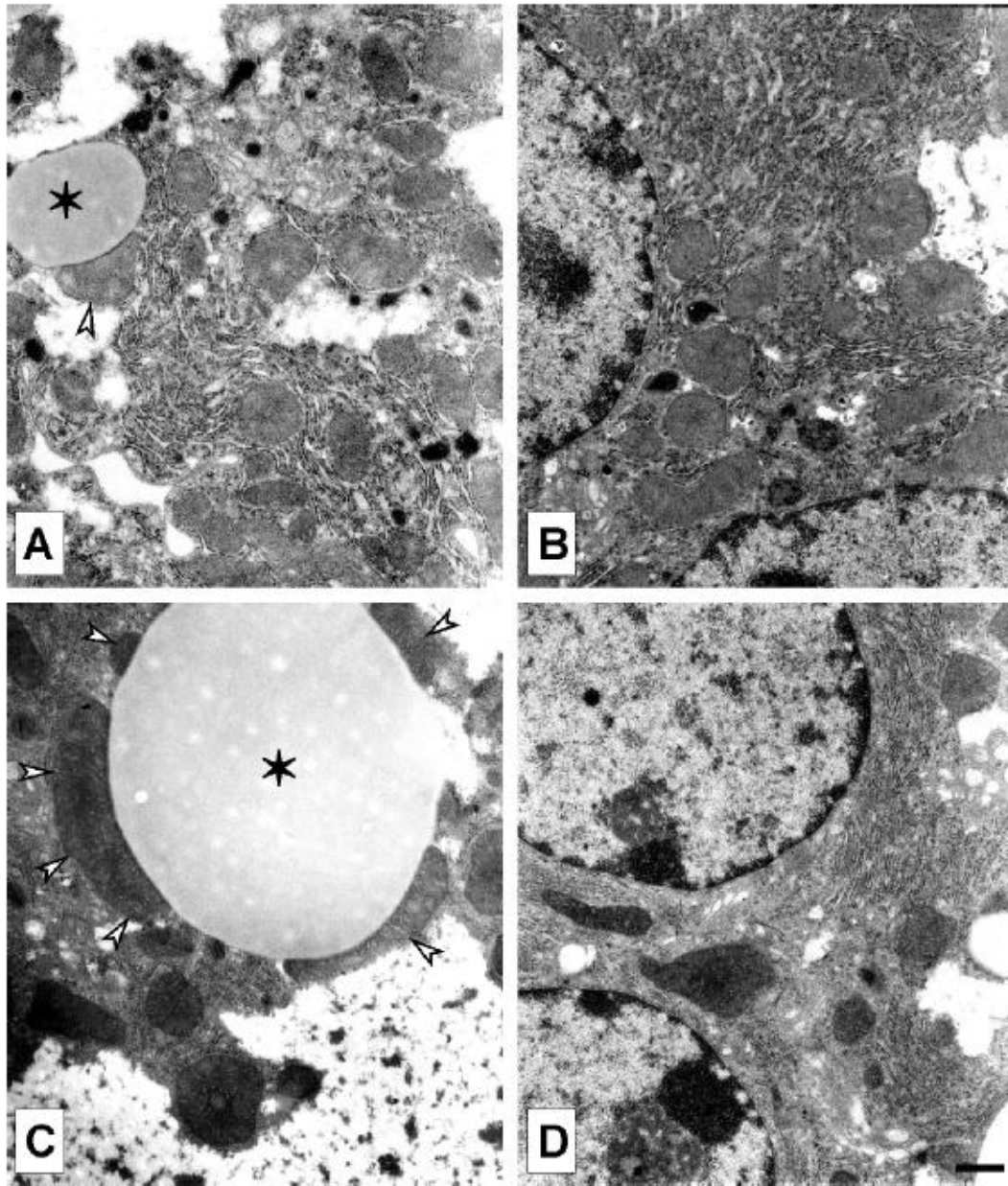
	WT	eNOS-KO
mitochondria (% of cytosolic volume)		
zone 1	28.27 ± 1.05	17.07 ± 0.99*
zone 3	29.80 ± 0.80	37.06 ± 1.34
zone 1 + zone 3	29.03 ± 0.93	27.07 ± 1.12
CS ($\mu\text{Mol mg}^{-1} \text{min}^{-1}$)	0.0574 ± 0.0074	0.0454 ± 0.0023*
KI+III ($\mu\text{Mol mg}^{-1} \text{min}^{-1}$)	0.276 ± 0.023	0.163 ± 0.011*
CS/KI+III	0.208 ± 0.021	0.279 ± 0.019*

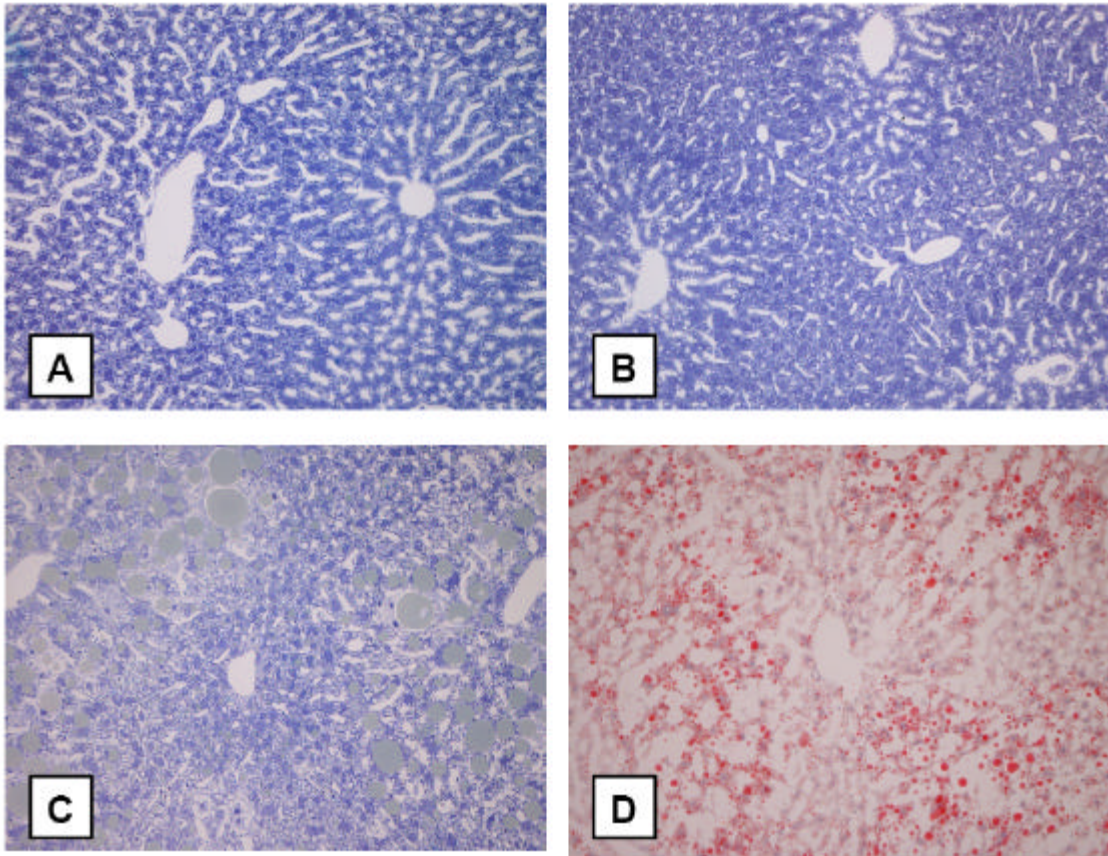
Effect of eNOS-derived NO on the distribution and enzymatic pattern of mitochondria in liver. The distribution of mitochondria was analyzed on the base of electron micrographs. Three animals per group were evaluated for this investigation. For the determination of the activities of CS and KI+III liver homogenates were prepared. Five livers were used for each group. The data are presented as mean ± SEM. Differences between parameters of eNOS-KO and WT mice were analysed by applying unpaired Student's *t* test. *difference between WT and eNOS-KO mice is significant with $p < 0.05$.

	WT	<i>eNOS-KO</i>
glucose (mmol/l)	9.44 ± 0.71	7.63 ± 0.69*
triacylglycerol (mmol/l)	1.14 ± 0.36	1.44 ± 0.30
<i>insulin</i> (ng/ml)	1.68 ± 0.51	0.63 ± 0.23*

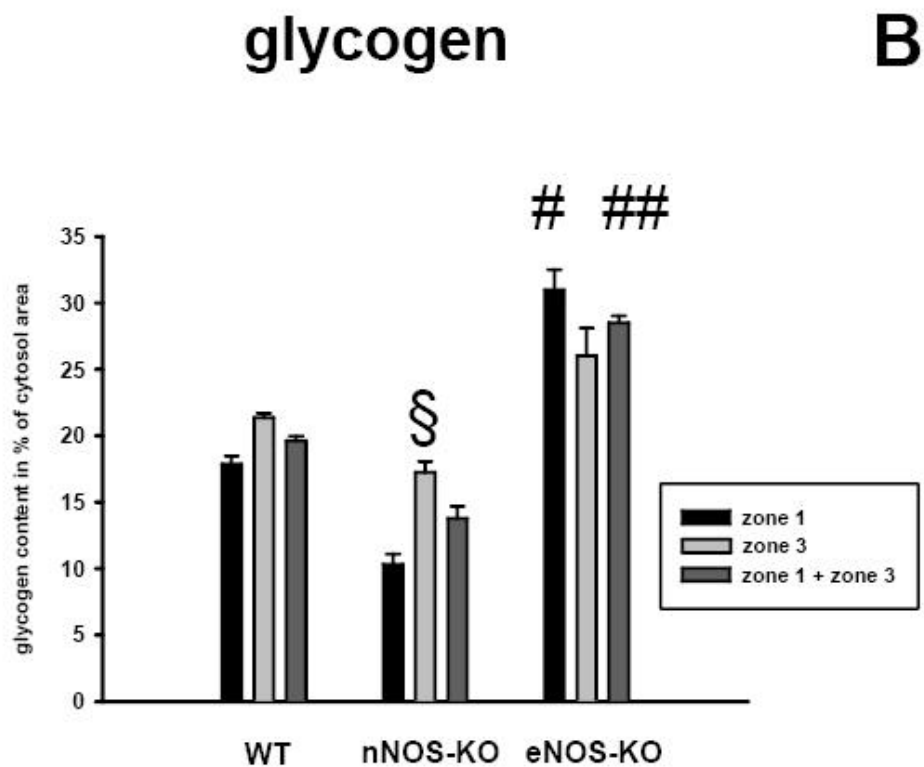
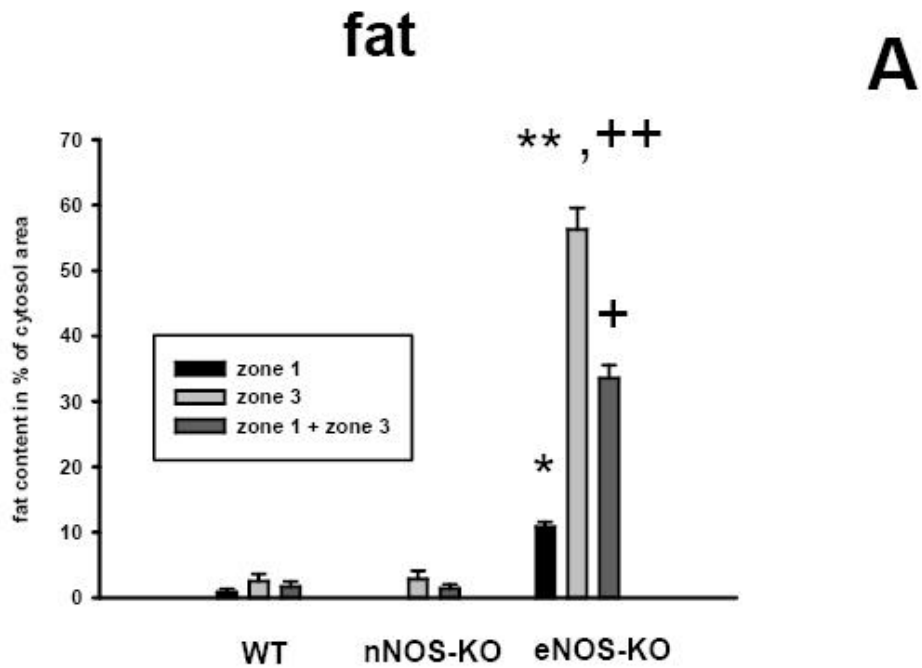
Effect of eNOS-derived NO on serum levels of glucose, triacylglycerol, and insulin.

Serum samples from trunk blood were collected at sacrifice. Five animals of each group were analyzed. The data are presented as mean ± SEM. Differences between parameters of eNOS-KO and WT mice were analysed by applying unpaired Student's *t* test. *difference between WT and eNOS-KO mice is significant with $p < 0.05$.

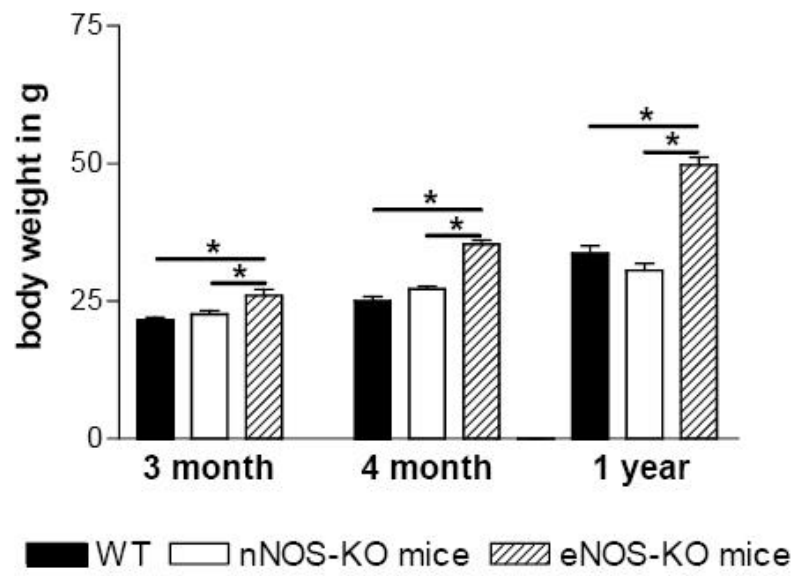




ACCEPTED







ACCEPTED